American Mineralogist, Volume 80, pages 483–490, 1995

Mg self-diffusion in pyrope garnet

CRAIG S. SCHWANDT,* RANDALL T. CYGAN, HENRY R. WESTRICH
Geochemistry Department, Sandia National Laboratories, Albuquerque, New Mexico 87185-0750, U.S.A.

ABSTRACT

Mg self-diffusion coefficients were experimentally determined for natural pyrope-almandine garnet in a 1 atm CO-CO_2 gas-mixing furnace at temperatures of 800–1000 °C. Diffusion couples consist of polished garnet crystals covered with a thin film of enriched stable-isotope oxide produced by high-vacuum thermal evaporation of ^{25}MgO. Experiments conducted at quartz + fayalite + magnetite f_{O_2} provide ^{25}Mg diffusion coefficients as a function of temperature. The short diffusion penetration profiles (<2000 Å) in the garnet were analyzed by secondary ion mass spectrometry and ion microprobe using a depth profiling technique. The resulting self-diffusion coefficients are lower than the low-temperature data of other experimental studies. The activation energy and preexponential term derived from the experimental diffusion coefficients obtained at 800, 900, and 1000 °C are given by $E_a = 294 \pm 51$ kJ/mol and $\log D_0 = -8.0 \pm 2.3$ m²/s. The activation energy is similar to that obtained from other cation diffusion studies of garnet at low temperature. Additional experiments conducted at 1000 °C to determine ^{25}Mg diffusion as a function of f_{O_2} and composition are inconclusive. However, comparison of the results of the present study with previous data indicates that f_{O_2} and mineral composition are important factors for the diffusion of cations in garnet.

INTRODUCTION

Determination of accurate crystallization cooling rates (Buening and Buseck, 1973; Vance and O'Nions, 1990; Tilton et al., 1991; Getty and Gromet, 1992; Burton and O'Nions, 1992) and tectonic uplift rates (e.g., Lasaga, 1983; Bohlen, 1987; Crowley and Spear, 1987; Medaris et al., 1990; Burton and O'Nions, 1991; Crowley, 1991; Frost and Tracy, 1991; Sharp and Essene, 1991) is often based on compositional zoning and the diffusion coefficients of cations for minerals such as garnet. Garnet commonly exhibits compositional zoning because diffusion of cations through its structure is sluggish relative to other minerals. As a result, many researchers (Elphick et al., 1985; Loomis et al., 1985; Chakraborty and Ganguly, 1991, 1992) have examined cation diffusion in garnet by conducting laboratory experiments at temperatures >1100 °C. The resulting data then require extrapolation to temperatures typical of crustal metamorphic systems. However, extrapolation of diffusion data obtained at 1100–1300 °C to 600–1000 °C may be inappropriate, as there may be significant changes in the mechanisms and activation energies of diffusion in these temperature ranges (e.g., Lasaga, 1980; Cygan and Lasaga, 1985; Shewmon, 1989).

Anneal temperatures above 1100 °C were used in these studies because the higher temperatures allow for sufficiently large (≈20 μm) experimental diffusion-penetration distances that can be measured with an electron microprobe. For microprobe analyses, the excitation volume for X-rays generated by even a 1 μm diameter electron beam is a few cubic micrometers. Therefore, previous diffusion experiments on garnet (e.g., Freer, 1979; Elphick et al., 1985; Chakraborty and Ganguly, 1992) typically utilized mineral–mineral or mineral–sintered oxide sandwiches as diffusion couples. The extent and distance of diffusional penetration was measured along cross sections of the diffusion couple. Using this approach, investigations of cation diffusion in garnet are limited to experiments at temperatures above 1100 °C in order to achieve sufficient diffusional penetration.

Conducting meaningful cation diffusion experiments on garnets at temperatures <1100 °C and with practical durations for the anneal time (no greater than a couple of months) requires an analytical technique with very fine spatial resolution. We therefore utilized an ion microprobe and secondary ion mass spectrometry (SIMS) to examine the samples from our experiments. The depth-profiling mode of the ion microprobe provides a spatial resolution that is several orders of magnitude smaller than that associated with the electron microprobe. Using SIMS for depth profiling, material is eroded from the sample in a plane parallel to the interface of the diffusion couple. Secondary ions, generated by the ablation process, are subsequently analyzed by a mass spectrometer, providing compositional information as a function of depth with tens of ångströms spatial resolution.

Using diffusion couples that consist of a film of enriched ^{25}MgO deposited on polished garnet surfaces, we

* Present address: NASA-NRC, Johnson Space Center, SN4, Houston, Texas 77058-3696, U.S.A.

0003–004X/95/0506–0483$02.00

TABLE 1. Compositions of garnet types

Oxide	A	B	C	Uncertainty ($\pm 1\sigma$)
SiO_2	40.88	41.41	40.00	0.17
Al_2O_3	25.93	24.70	24.29	0.33
MgO	17.78	19.96	21.17	0.25
FeO	8.95	8.83	7.79	0.15
MnO	1.02	0.60	0.00	0.07
CaO	5.43	4.50	5.17	0.21
Cr_2O_3	0.00	0.00	1.57	0.50
Total	99.99	100.00	99.99	
	End-member fraction*			
Mg/(Mg + Fe)	0.78	0.80	0.83	
Pyrope	0.66	0.70	0.72	
Almandine	0.18	0.18	0.15	
Spessartine	0.02	0.01	0.00	
Grossular	0.14	0.11	0.13	

Note: representative analyses obtained by standardless energy-dispersive X-ray normalized to 100%.
* Based on 12 O atoms.

measured, by SIMS, the self-diffusion of ^{25}Mg in chemically homogeneous, natural Mg-rich garnet (pyrope) at temperatures of 800–1100 °C under controlled f_{O_2} conditions. Self-diffusion is the migration of an isotope due to an isotopic gradient rather than a chemical gradient (e.g., Freer, 1981; Andersson et al., 1989; Sheng et al., 1992).

EXPERIMENTAL APPROACH

The Mg-rich garnet crystals used in these experiments were collected from a diatreme at Buell Park, Arizona (O'Hara and Mercy, 1966; Switzer, 1977). Three slightly different garnet compositions were used (Table 1). The majority of experiments used type A garnets and were conducted at different temperatures (800–1100 °C) and at f_{O_2} slightly lower than that defined by the quartz + fayalite + magnetite (QFM) buffer (log $f_{O_2} \approx -15$ to -11). QFM conditions were chosen so that the Fe^{3+}-Fe^{2+} ratio would remain low and approximate the conditions of crustal metamorphism. Experiments investigating f_{O_2} dependence at 1000 °C used type B garnets. The type C garnets are identical to those used in the study of Cygan and Lasaga (1985).

Diffusion for an isometric mineral, such as garnet, is defined by a single diffusion coefficient (Nye, 1957). Therefore, the pyrope garnet crystals were randomly cut with a wafering saw into small slabs ($\approx 4 \times 4 \times 1$ mm) and polished using diamond pastes down to 1 μm. A final stage of polishing used 0.06 μm colloidal silica. The polished samples provide a suitable surface for the application of the diffusion source material.

The polished garnet samples were preannealed for 24 h at the temperature and f_{O_2} conditions to be used for each of the diffusion experiments. This was done to equilibrate the bulk point-defect structure of the samples to the conditions expected for each diffusion experiment. The preannealing process should also remove, or at least minimize, the surface defects generated by the polishing process, although Ryerson et al. (1989) demonstrated that preannealing and chemical polishing had minimal effect on the results of diffusion experiments in olivine. The preannealing of the samples and the diffusion experiments were conducted in a vertical muffle-tube furnace at atmospheric pressure. Oxygen fugacity inside the furnace is controlled by continuous flow of a CO-CO_2 gas mixture (Deines et al., 1974) and is monitored by a solid-electrolyte sensor mounted 2 cm above the sample in the center of the 15 cm hot zone of the furnace. Temperature and f_{O_2} gradients near the sample are expected to be insignificant with this experimental arrangement.

After preannealing, the garnet samples were coated with a thin film ($\approx$1000 Å) of $^{25}MgO_x$ ($x < 1$) using high-vacuum thermal evaporation of ^{25}MgO powder (Schwandt et al., 1993); the ^{25}Mg is enriched to 94.5%. The resulting diffusion couples (oxide-garnet) were then used for the self-diffusion experiments by annealing the couples at each of the following temperatures: 800, 900, 1000, 1050, and 1100 °C. Multiple experiments were conducted for different durations at each temperature. The range of experimental anneal time is from 1.5 h for experiments at 1000 °C to 3 months at 800 °C (Table 2).

A Cameca IMS 4f ion microprobe was optimized for depth-profile analysis of the samples resulting from the diffusion experiments. Each analysis consisted of rastering a 30–50 μm diameter, 75 nA O beam, with acceleration of 10 kV, over a 150 × 150 μm area of the sample surface. Optimal analysis conditions included a 20 eV energy window, a 50 V sample-bias offset, a 400 μm field aperture, and a 150 μm contrast aperture. The rate of primary beam penetration into the sample was determined by sputtering several craters into the thin film and several craters into garnet for known times. Subsequently, the depths of these craters were measured by contact-stylus profilometry. Replicate measurements were made to estimate reproducibility and precision. No discernable difference between the sputter rates for the thin film and garnet was observed; a linear sputter rate of 1.00 ± 0.05 Å/s was determined from this analysis. The crater depths were shallow enough that primary beam intensity was not affected by the field of secondary ions nor by crater sidewall effects.

Counts of secondary ions, or intensities, extracted after impact of the primary O^- beam with the garnet sample were collected as a function of time for ^{24}Mg, ^{25}Mg, ^{26}Mg, ^{27}Al, ^{28}Si, ^{40}Ca, ^{47}Ti, ^{55}Mn, and ^{56}Fe. During the sputtering process the instrumental sensitivity dramatically increased as the primary ion beam approached the diffusion couple interface and then typically decreased beyond (Wilson et al., 1989). Once the interface of the thin film–garnet sample was identified (see below), the diffusional penetration distance was calculated by multiplying the remaining analysis time by the sputter rate. We observed improved reproducibility of the depth profiles by using the same ion microprobe operating conditions for all analyses and then calculating the crater depths on the basis of the determined sputtering rate. Analysis of an unannealed diffusion couple yields a ^{25}Mg fraction of 0.945

TABLE 2. Self-diffusion coefficients for ^{25}Mg in pyrope garnet

Garnet type	Anneal t (h)	log f_{O_2}	Diffusion coefficient (m^2/s) 1100 °C	1050 °C	1000 °C	900 °C	800 °C
A	1.5	−11.6			7.8×10^{-20}		
A	3	−11.5			4.3×10^{-20}		
A	6	−11.4			4.1×10^{-20}		
A	6	−10.0	(3.03×10^{-18})*				
A	12	−11.4			2.2×10^{-20}		
A	24	−10.0	(6.57×10^{-19})*				
A	24.2	−10.4		(2.92×10^{-19})*			
A	48	−12.3			4.5×10^{-21}		
A	96.5	−12.3			1.25×10^{-21}		
B	72	−9.8			3.2×10^{-21}		
B	72	−11.2			5.1×10^{-21}		
B	72	−14.0			9.5×10^{-21}		
B	72	−16.1			7.9×10^{-21}		
C	72	−11.2			2.0×10^{-21}		
A	144	−13.0				3.5×10^{-21}	
A	286.75	−13.1				3.2×10^{-21}	
A	603.6	−13.1				1.3×10^{-21}	
A	1771	−15.2					8.6×10^{-23}
A	2130	−15.2					7.4×10^{-23}
Infinite time value					5.75×10^{-21}	1.26×10^{-21}	3.55×10^{-23}
log D					−20.24	−20.90	−22.45
Error					±0.28	±0.24	±0.27

Note: each D is the mean of three replicate analyses; the 1σ uncertainty values are 8% (relative).
* Apparent D values; garnets have reacted (see text).

in agreement with the enrichment factor of the ^{25}MgO used for production of the thin film. This confirms that there is no significant isotope fractionation during the evaporation process to create the thin film or during the SIMS analysis.

The intensity vs. depth profiles obtained by the ion microprobe exhibit complex zoning patterns within the first several hundred ångströms of the MgO outer surface. This behavior is the result of the nonsteady-state sputtering process (Wilson et al., 1989) and the interference of the isotope-enriched oxide layer as the garnet is sputtered into. Additional factors, including knockdown effects and surface roughness, lead to a broadening of the oxide-garnet interface as defined by the mass intensities (Schwandt et al., 1993). In order to determine properly the position of this interface, a critical parameter for fitting the data to a diffusion model, we chose to monitor the $^{25}Mg/^{27}Al$ value, which is characterized by a large discontinuity at the thin film–garnet interface. The raw ^{25}Mg intensity data are reduced to $^{25}Mg/^{28}Si$ values in order to evaluate the true variation in the ^{25}Mg intensity as a function of depth. The ^{28}Si, acting as a component of constant concentration, is used as a reference to reduce or eliminate any variations in the mass intensities resulting from the mechanics of the ion microprobe analysis (see Giletti and Casserly, 1994). The $^{25}Mg/^{28}Si$ depth profile is used to calculate the diffusion coefficient.

The application of thin films to create the oxide-garnet diffusion couple provides an alternative and much-improved experimental approach for evaluating diffusion coefficients of cations in minerals using the ion microprobe. In contrast, an inhomogeneous distribution of the enriched isotope, typically deposited from solution as a precipitated salt, and the associated surface roughness often lead to difficulties in the depth-profile analysis with the ion microprobe (Cygan and Lasaga, 1985; Chakraborty et al., 1992; Giletti and Casserly, 1994). The use of the homogeneous thin film as the source of the isotope tracer, in contrast, provides an initially homogeneous and smooth oxide surface that is slightly modified by the diffusion anneal (Schwandt et al., 1993). The depth profiles that are obtained are highly reproducible with a precision of approximately 5%. We obtain diffusion coefficients that typically vary by <8% for these multiple analyses (Table 2).

Although the thin film approach ensures excellent precision in the reproducibility of the depth-profile analyses, the permanency of the oxide layer and the need to sputter through it lead to an artificial time dependence in the calculated diffusion coefficients (Schwandt et al., 1993). Our recent measurements of Ca diffusion in garnet using a removable $^{44}Ca(OH)_2$ thin film demonstrate the lack of any time dependence; the hydroxide thin film is readily dissolved in water to provide a clean garnet surface for the ion microprobe analysis (unpublished data). However, in the depth-profile analysis of the MgO thin film–garnet samples we observe a trend in the calculated diffusion coefficients that exhibits a linear log D vs. $1/t$ behavior. This empirical observation is related to several factors associated with the ion sputtering process of the composite-diffusion couple and the depth of the diffusional penetration (Schwandt et al., 1993). The limiting D values reported in Table 2 are those obtained by the infinite time intercepts of the best fits ($\log D \propto 1/t$). The associated uncertainties in the log D values are obtained from the residuals associated with the linear regression.

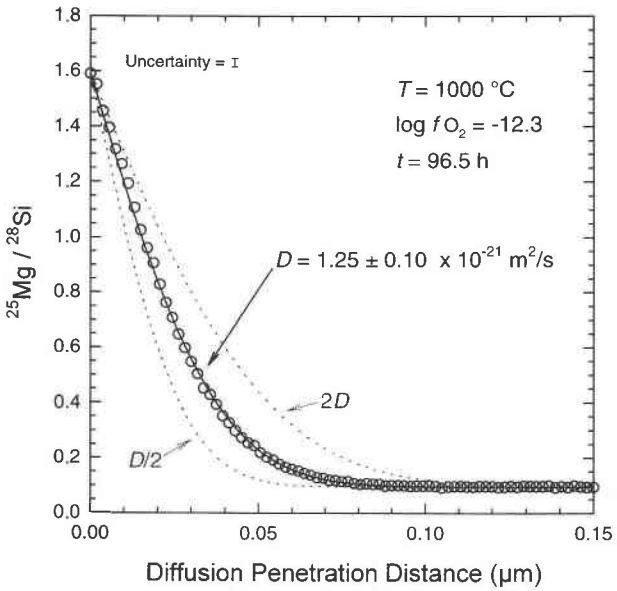

Fig. 1. The value of $^{25}Mg/^{28}Si$ plotted against diffusion-penetration distance for a 1000 °C experiment. Open circles represent a measured diffusion-penetration profile. The solid line represents the best fit to the diffusion model for the measured profile. Dotted lines represent model profiles using half and twice the best-fit value of D.

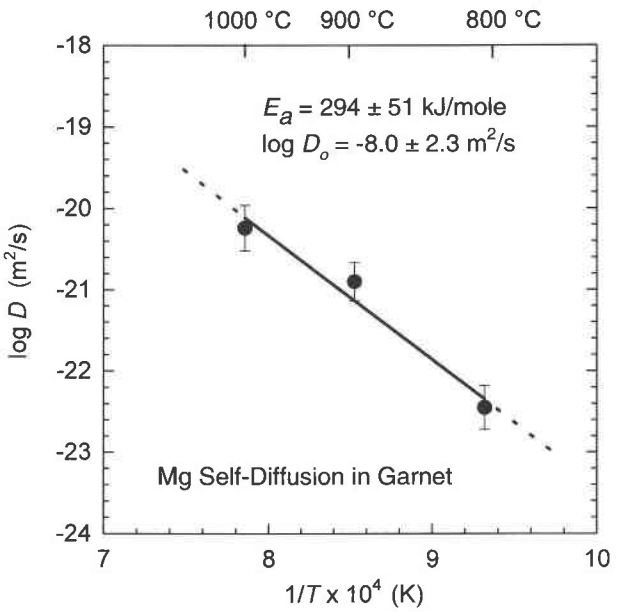

Fig. 2. Arrhenius plot of the experimental ^{25}Mg self-diffusion values at QFM f_{O_2} conditions. The best fit to the measured diffusion coefficients, used to obtain the activation energy and preexponential term, is denoted by the solid line.

Results

After conducting the diffusion experiments and obtaining the depth profiles with the ion microprobe, diffusion coefficients are obtained with a diffusion model that satisfies both the initial condition and the boundary conditions of the experimental anneal and provides the best fit to the measured data. We use the semi-infinite medium solution to the Fickian diffusion equations obtained by Crank (1975) as representative of our experimental conditions:

$$C_x = C_s + (C_b - C_s)\mathrm{erf}\left(\frac{x}{\sqrt{4Dt}}\right) \quad (1)$$

where C_x is the ^{25}Mg concentration (in terms of $^{25}Mg/^{28}Si$) at position x in the garnet, C_s is the surface concentration that is maintained during the diffusion anneal, C_b is the bulk concentration of the garnet, D is the ^{25}Mg self-diffusion coefficient, and t is the duration of the experimental anneal. This solution assumes an initially homogeneous distribution of ^{25}Mg throughout the garnet.

A nonlinear least-squares fitting routine that allows C_x, C_b, and D to vary is used to fit Equation 1 to the $^{25}Mg/^{28}Si$ data for each experiment. An example of the best fit of the model and the extent to which the diffusion coefficient can be determined are provided in Figure 1. Uncertainties (1σ) associated with individual curve fit determinations for D are about 2% (relative). Triplicate analyses of individual experiments indicate a maximum uncertainty in precision for the D values of about 8% (relative) (Table 2).

To ensure the integrity of the samples after they were annealed, all the samples were examined optically, with a scanning electron microscope (SEM), and by X-ray diffraction analysis. The samples held at 1000 °C and at lower temperatures show no SEM or X-ray diffraction evidence of breakdown and remain optically isotropic. However, the 1050 and 1100 °C samples suffered from breakdown reactions as these samples became opaque and black. The X-ray diffraction analysis revealed that the surface of the annealed garnet consists of a combination of garnet, periclase, enstatite, augite, anorthite, hercynite, and magnetite. The apparent diffusion coefficients resulting from these high-temperature experiments are a few orders of magnitude larger than expected by extrapolation of the lower temperature values (Table 2).

Discussion

The temperature dependence of the diffusion coefficient can be presented in terms of an Arrhenius plot (Fig. 2) where log values of D are plotted against the reciprocal of the anneal temperature. Arrhenius relationships are typically defined as in Equation 2, which can be rewritten in a linear fashion as Equation 3:

$$D = D_0 e^{\frac{-E_a}{RT}} \quad (2)$$

$$\log D = \log D_0 - \frac{E_a}{2.3026RT} \quad (3)$$

where $\log D_0$ is the value of the intercept when $T = \infty$, the frequency factor D_0 is expressed in units of squared meters per second, T is the temperature in Kelvin, and R is the gas constant. The slope of the best-fit line to

Equation 3 provides the value of E_a, the activation energy, expressed in kilojoules per mole. A linear least-squares fit of the ^{25}Mg data for pyrope garnet of composition A at QFM f_{O_2} provides log $D_0 = -8.0 \pm 2.3$ m^2/s ($D_0 = 1.0 \times 10^{-8}$ m^2/s) and $E_a = 294 \pm 51$ kJ/mol. The uncertainties for these values were obtained by standard error-propagation techniques incorporating the uncertainties of the ion microprobe analysis, the fitting of the data to the diffusion model, the infinite time extrapolations, and the Arrhenius fit.

In Figure 3, the Mg self-diffusion data are presented in an Arrhenius plot with previous cation diffusion studies for garnet, without correction for the different P and f_{O_2} conditions of each of the experiments. Comparison of the data by normalization to a common set of conditions can be misleading because, in addition to the differences in P, T, and f_{O_2}, there are differences in the compositions of the garnets and the experimental techniques. Without conducting experiments on a broad range of compositions using the same technique, the effect of garnet composition cannot be isolated from effects that may be technique dependent. Differences in the activation energies are evident by comparison of the slopes of the Arrhenius lines (Fig. 3). The diffusion coefficients determined for this study are considerably lower than those of previous studies performed at similar low temperatures, the primary reason for the discrepancy being the difference in f_{O_2}. Nonetheless, one would expect the Chakraborty et al. (1992 personal communication) data to exhibit the slowest diffusion rates resulting from the reduced f_{O_2} conditions (near WM buffer). Because of the possibility of changing diffusion mechanisms, caution must be used when comparing the extrapolation of high-temperature data to lower temperatures. It is interesting to note, however, that the Loomis et al. (1985) data for Mg tracer diffusion obtained from an almandine-spessartine diffusion couple at high temperature and high pressure (4 GPa) is in excellent agreement with the ^{25}Mg self-diffusion data of Cygan and Lasaga (1985) obtained at low temperature once pressure and f_{O_2} corrections are performed (Chakraborty and Ganguly, 1991).

Volume diffusion of a cation through a mineral crystal structure is controlled by the occurrence, type, and abundance of point defects. Lasaga (1981) reviewed intrinsic vs. extrinsic behavior and the importance of defects to diffusion. In the intrinsic region at higher temperatures, point defects are thermally generated and controlled, providing the temperature dependence of diffusion. At lower temperatures, cation impurities (for example, multivalent elements) influence the defect structure to a larger extent than does the temperature, thereby defining extrinsic behavior. On an Arrhenius plot of log D vs. $1/T$, steep slopes characterize intrinsic behavior and shallow slopes characterize extrinsic behavior. We see no evidence that line or planar defects contribute to cation diffusion in our experiments. One would expect significantly enhanced diffusion if these long-range defects contributed to the bulk diffusion.

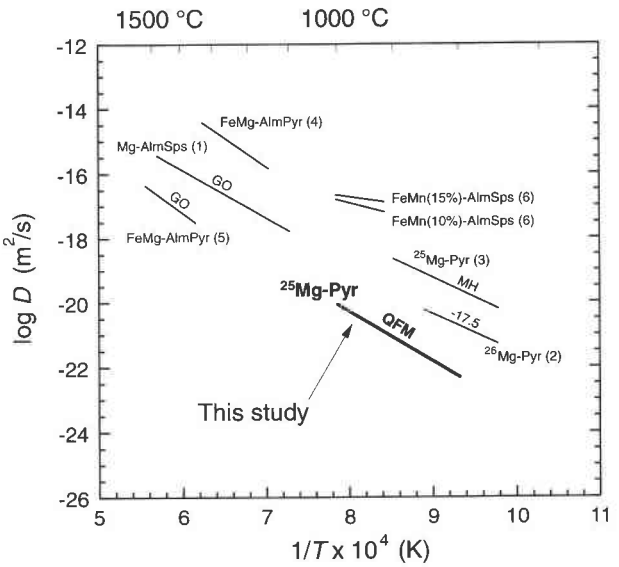

Fig. 3. Arrhenius compilation of the experimental data for Mg, Fe, and Mn diffusion in garnet: 1 = Chakraborty and Ganguly (1992); 2 = Chakraborty et al. (1992) and Chakraborty (personal communication); 3 = Cygan and Lasaga (1985); 4 = Duckworth and Freer (1981); 5 = Elphick et al. (1985); 6 = Freer (1979). No corrections were made for differences in composition, pressure, or f_{O_2}. Experimental f_{O_2} conditions (solid-state buffer assemblages) are noted for each line when reported in the original study.

Fe-Mg interdiffusion may be enhanced by Fe^{3+}, and the fraction of Fe^{3+} to Fe^{2+} is dependent on f_{O_2} conditions. As an example, the Fe-Mg interdiffusion coefficient in olivine for the extrinsic region was found to be proportional to $f_{O_2}^{1/6}$ (Buening and Buseck, 1973). The olivine data are consistent with a simple Fe oxidation-vacancy defect equilibrium model (Buening and Buseck, 1973). The oxidation of Fe^{2+} to Fe^{3+} in the octahedral site of olivine is accompanied by the formation of octahedral site vacancies that enhance the diffusion of these divalent cations (Lasaga, 1981). The defect structure in garnet is more complicated than that in olivine because rather than two octahedral sites the garnet structure possesses an octahedral site and an eightfold-coordinated site (Novak and Gibbs, 1971; Cygan and Lasaga, 1985). In garnet, Mg, Fe^{2+}, Mn^{2+}, and Ca normally occupy the eightfold-coordinated sites and Al normally occupies the octahedral sites. Therefore, with these structural differences in mind, the oxidation/vacancy defect mechanism that provides the proportionality of D with $f_{O_2}^{1/6}$ in olivine may be more complicated for cation diffusion in garnet. The Fe^{3+} or Mn^{3+} may move, or order, into the octahedral sites for size and charge reasons. The substitution of Fe^{3+} or Mn^{3+} into the octahedral site requires exchange for Al. These combined reactions may possibly lead to an f_{O_2} dependence of something other than $\frac{1}{6}$ for diffusion in garnet.

Experiments at 1000 °C and different f_{O_2} conditions revealed no dependence of D on f_{O_2} (Table 2); the vari-

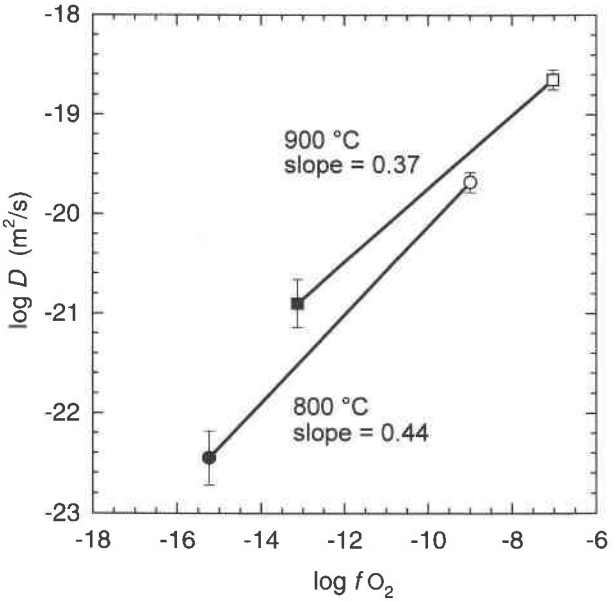

Fig. 4. Plot of log D vs. log of the f_{O_2}. The solid and open symbols represent the Mg self-diffusion data of the present study (QFM buffer) and that of Cygan and Lasaga (1985) (HM buffer), respectively. The slope values represent the exponent in the $D \propto f_{O_2}^n$ relation.

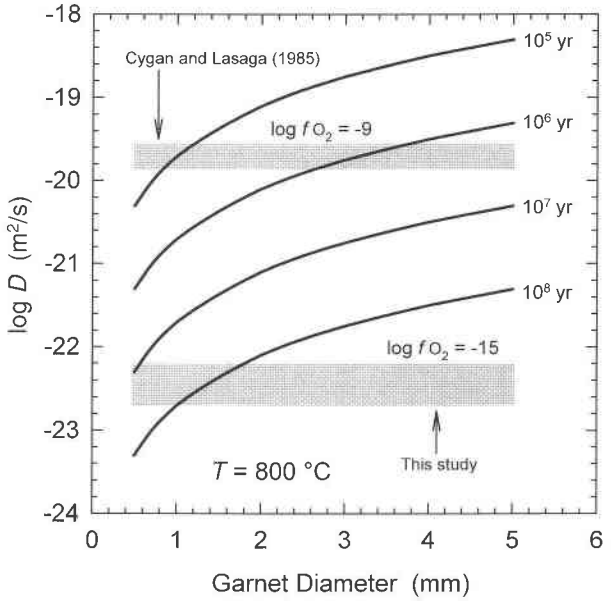

Fig. 5. Plot of log D vs. garnet diameter describing time required for chemical homogenization of an initially zoned garnet. Solid lines represent the approximate time required for chemical homogenization of a garnet at 800 °C on the basis of a mean distance of diffusion. The time required for homogenization is a function of the f_{O_2} conditions associated with the garnet. The width of the gray bands represents the uncertainty in the log D values.

ation in D is within the uncertainty determined for the QFM diffusion result. This result is unexpected given the f_{O_2} dependence for cation diffusion in olivine observed by Buening and Buseck (1973) and others. One possible explanation for this behavior is that these experiments were all conducted under identical anneal times and may be affected by analytical complications, as previously discussed. Nonetheless, we can compare the ^{25}Mg self-diffusion data of this study, obtained at QFM f_{O_2}, with those of Cygan and Lasaga (1985), obtained at HM f_{O_2} conditions. This comparison is presented in the log D vs. log f_{O_2} plot of Figure 4, which exhibits slopes ranging from 0.31 to 0.50 taking into account the uncertainty (1σ) in the log D values. The garnets in the Cygan and Lasaga (1985) study contain approximately 1.5 wt% Cr but otherwise are compositionally the same as the garnets in this study. Therefore, any oxidation state-vacancy mechanism that might be influencing cation diffusion in garnet appears to be enhanced relative to that observed in olivine (slope of 0.17). Diffusion experiments conducted under more oxidizing conditions (72 h at HM buffer) were unsuccessful because of the breakdown of the garnet. The upper f_{O_2} stability limit of the garnets of this study occurs between log $f_{O_2} = -8$ and -9.75 for temperatures of 1000 °C and is similar to that calculated by Anovitz et al. (1993) on the basis of calorimetry experiments of a synthetic end-member almandine.

The defect structure of garnet is not solely a function of f_{O_2} conditions but is also a function of composition, especially the Fe content. For constant f_{O_2} conditions the Fe^{3+} to Fe^{2+} ratio is fixed, and the amount of Fe^{3+} or other multivalent cations that can affect the defect structure is dependent on the composition. Experiments at 1000 °C that were conducted to test for a compositional dependence of D revealed no significant correlation. However, the compositional variations in this investigation are small (<3 mol% almandine) relative to the amount of Fe in all three types of pyrope (15–20 mol% almandine). Alternatively, the experiments conducted at 1000 °C may be near the transition from an extrinsically to an intrinsically dominated process. In the intrinsic region compositional differences would be of minor importance. The present data set is still too small to determine unequivocally the controlling mechanisms at temperatures below 1000 °C, although the activation energy, relatively small, suggests that diffusion is controlled extrinsically rather than intrinsically.

Given the importance f_{O_2} and composition have on cation diffusion in silicate minerals, we suggest that they are the primary factors controlling differences observed in the Mg diffusion at low temperature in garnet (Fig. 3). The garnets used in Chakraborty et al. (1992) have significantly higher Fe contents ($Prp_{21}Alm_{73}Sps_1Grs_5$ and $Prp_{50}Alm_{38}Sps_2Grs_{10}$) relative to Mg than the garnet composition ($Prp_{66}Alm_{18}Sps_2Grs_{14}$) of this study. Although not presented in Figure 3, the higher Fe-content garnet of Chakraborty et al. (1992) provides a ^{26}Mg self-diffusion coefficient that is approximately 80% larger than that of the low Fe-content garnet. This trend suggests that Fe

content is an important factor, although more experiments are needed to identify fully the exact compositional and f_{O_2} relationships.

Petrologic implications

Diffusion coefficients significantly impact the results of several types of modeling, including geochronology (e.g., Vance and O'Nions, 1990; Tilton et al., 1991; Getty and Gromet, 1992; Burton and O'Nions, 1992), chemical equilibrium for mineral phases (e.g., Velde et al., 1991; Thomson, 1992), and pressure-temperature-time path and tectonic reconstructions (e.g., Bohlen, 1987; Crowley and Spear, 1987; Medaris et al., 1990; Burton and O'Nions, 1991; Crowley, 1991; Frost and Tracy, 1991; Sharp and Essene, 1991). In each case, the diffusional processes and the magnitude of the diffusion coefficient are the critical factors in support of the theoretical or conceptual model.

For example, the duration of a metamorphic event can be estimated from the extent of compositional homogenization of zoned garnets. If one considers the mean distance of diffusional penetration to be $x = (4Dt)^{1/2}$ as given by Crank (1975), where x equals the radius of a garnet, then the time required for homogenization of the compositional zoning of a garnet held at a given temperature varies considerably depending on the diffusion coefficient (Fig. 5). In this example, a difference in time of two-and-a-half orders of magnitude is required, depending on the f_{O_2} conditions, for grains of a given size at 800 °C to homogenize. Even at 800 °C, diffusional adjustment of compositional profiles may require considerably more time than previously thought. These data suggest that volume diffusion in garnet, at least for Mg diffusion in pyrope garnets, may not be an important process for the formation of compositional zoning in amphibolite grade (500–600 °C) garnet.

The diffusion data of this study can also be used to estimate closure temperature and cooling rates associated with compositional zoning in garnet. During cooling after thermal metamorphism, the compositional profile can be modified in response to changing conditions until the temperature drops to the closure temperature, T_c, below which volume diffusion is not a viable process and compositions remain fixed. Dodson (1973) derived an expression that describes the relationship of closure temperature (volume averaged), cooling rate, and diffusion:

$$\frac{E_a}{RT_c} = \ln\left(-\frac{ART_c^2D_0}{a^2E_as}\right) \quad (4)$$

where E_a is the diffusion-activation energy, R is the gas constant, A is a geometric factor, which is equal to 55 for spheres, D_0 is the diffusion-frequency factor, a is the radius of a spherical grain, and s is the change in temperature with time (cooling rate, a negative value). Ehlers and Powell (1994) have recently generalized this expression to account for compositional exchange and modal effects, however the original Dodson (1973) equation is suitable for the following discussion. Using this equation and the Arrhenius values from the present study and Cygan and Lasaga (1985), we obtain significantly different closure temperatures for a given cooling rate under the different f_{O_2} conditions (Fig. 6). For example, a 4 mm diameter garnet cooling at a rate of 10 °/m.y. has a closure temperature of 890 °C at QFM, whereas at HM conditions the closure temperature is reduced to 680 °C. This difference in closure temperature reflects the slower diffusion data obtained under the relatively reducing experimental conditions of this study. Interestingly, the closure temperatures obtained for the QFM diffusion data at 10 °/m.y. are within about 50 °C of those for the HM data for a much faster cooling rate of 1000 °/m.y. Therefore, assessment of cooling rates on the basis of compositional zoning in garnet critically depends on the f_{O_2} conditions during metamorphism.

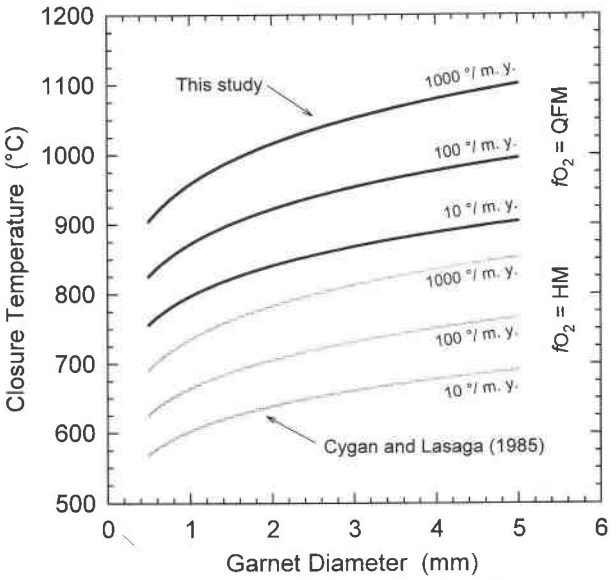

Fig. 6. Closure temperature plotted as a function of garnet diameter for three different cooling rates (Eq. 4). Using the diffusion data for the more oxidizing HM conditions leads to significantly lower closure temperatures than the temperatures derived using the data obtained from this study and the QFM f_{O_2} buffer.

Acknowledgments

We thank the Minerals Department of the Navajo Nation for permission to collect and use the garnet samples in this research. We acknowledge George Edgerly for his assistance with the thin film work and Graham Layne for his technical help with the ion microprobe analyses. We thank Sumit Chakraborty for sharing his low-temperature diffusion data with us prior to its publication. This paper was improved by the careful reviews of John Brady, Jiba Ganguly, and Eleanour Snow. The Geosciences Program of the U.S. Department of Energy, Office of Basic Energy Sciences, supported this research under contract DE-AC04-94AL85000 under contract to Sandia National Laboratories.

References cited

Andersson, K., Borchardt, G., Scherrer, S., and Weber, S. (1989) Self-diffusion in Mg_2SiO_4 (forsterite) at high temperature: A model case study for SIMS analyses on ceramic surfaces. Fresenius Zeitschrift für Analytish Chemie, 333, 383–385.

Anovitz, L.M., Essene, E.J., Metz, G.W., Bohlen, S.R., Westrum, E.F., and Hemingway, B.S. (1993) Heat capacity and phase equilibria of almandine, $Fe_3Al_2Si_3O_{12}$. Geochimica et Cosmochimica Acta, 57, 4191–4204.

Bohlen, S.R. (1987) Pressure-temperature-time paths and a tectonic model for the evolution of granulites. Journal of Geology, 95, 617–632.

Buening, D.K., and Buseck, P.R. (1973) Mg-Fe lattice diffusion in olivine. Journal of Geophysical Research, 78, 6852–6862.

Burton, K.W., and O'Nions, R.K. (1991) High-resolution garnet chronometry and the rates of metamorphic processes. Earth and Planetary Science Letters, 107, 649–671.

——— (1992) The timing of mineral growth across a regional metamorphic sequence. Nature, 357, 235–238.

Chakraborty, S., and Ganguly, J. (1991) Compositional zoning and cation diffusion in garnets. In Advances in Physical Geochemistry, 8, 120–175.

——— (1992) Cation diffusion in aluminosilicate garnets: Experimental determination in spessartine-almandine diffusion couples, evaluation of effective binary diffusion coefficients, and applications. Contributions to Mineralogy and Petrology, 111, 74–86.

Chakraborty, S., Rubie, D.C., and Elphick, S.C. (1992) Mg tracer diffusion in aluminosilicate garnets at 800 °C, 1 atm. and 1300 °C, 8.5 GPa. Eos, 73, 567.

Crank, J. (1975) The mathematics of diffusion, 414 p. Oxford University Press, Oxford, U.K.

Crowley, P.D. (1991) Thermal and kinetic constraints on the tectonic applications of thermobarometry. Mineralogical Magazine, 55, 57–69.

Crowley, P.D., and Spear, F.S. (1987) The *P-T* evolution of the Middle Köli Nappe Complex, Scandinavian Caledonides (68°N) and its tectonic implications. Contributions to Mineralogy and Petrology, 95, 512–522.

Cygan, R.T., and Lasaga, A.C. (1985) Self-diffusion of magnesium in garnet at 750° to 900°C. American Journal of Science, 285, 328–350.

Deines, P., Nafziger, R.H., Ulmer, G.C., and Woermann, E. (1974) Temperature and oxygen fugacity tables for selected gas mixtures in the system C-H-O at one atmosphere total pressure. Bulletin of the Earth and Mineral Sciences Experiment Station, 88, 129.

Dodson, M.H. (1973) Closure temperature in cooling geochronological and petrological systems. Contributions to Mineralogy and Petrology, 40, 259–274.

Duckworth, S., and Freer, R. (1981) Cation diffusion studies in garnet-garnet and garnet-pyroxene couples at high temperatures and pressures. Fifth Progress Report of Research Supported by Natural Environment Research Council (1978–1980), 18, 36–39.

Ehlers, K., and Powell, R. (1994) An empirical modification of Dodson's equation for closure temperature in binary systems. Geochimica et Cosmochimica Acta, 58, 241–248.

Elphick, S.C., Ganguly, J., and Loomis, T.P. (1985) Experimental determination of cation diffusivities in aluminosilicate garnets: I. Experimental methods and interdiffusion data. Contributions to Mineralogy and Petrology, 90, 36–44.

Freer, R. (1979) An experimental measurement of cation diffusion in almandine garnet. Nature, 280, 220–222.

——— (1981) Diffusion in silicate minerals and glasses: A data digest and guide to the literature. Contributions to Mineralogy and Petrology, 76, 440–454.

Frost, B.R., and Tracy, R.J. (1991) *P-T* paths from zoned garnets: Some minimum criteria. American Journal of Science, 291, 917–939.

Getty, S.R., and Gromet, L.P. (1992) Geochronological constraints on ductile deformation, crustal extension, and doming about a basement-cover boundary, New England Appalachians. American Journal of Science, 292, 359–397.

Giletti, B.J., and Casserly, J.E.D. (1994) Strontium diffusion kinetics in plagioclase feldspars. Geochimica et Cosmochimica Acta, 58, 3785–3793.

Lasaga, A.C. (1980) Defect calculations in silicates: Olivine. American Mineralogist, 65, 1237–1248.

——— (1981) The atomistic basis of kinetics: Defects in minerals. In Mineralogical Society of America Reviews in Mineralogy, 8, 216–319.

——— (1983) Geospeedometry: An extension of geothermometry. In S.K. Saxena, Ed., Kinetics and equilibrium in mineral reactions, p. 81–114. Springer-Verlag, New York.

Loomis, T.P., Ganguly, J., and Elphick, S.C. (1985) Experimental determination of cation diffusivities in aluminosilicate garnets: II. Multicomponent simulation and tracer diffusion coefficients. Contributions to Mineralogy and Petrology, 90, 45–51.

Medaris, L.G., Jr., Wang, H.F., Misar, Z., and Jelinek, E. (1990) Thermobarometry, diffusion modelling and cooling rates of crustal garnet peridotites: Two examples from the Bohemian Massif. Lithos, 25, 189–202.

Novak, G.A., and Gibbs, G.V. (1971) The crystal chemistry of the silicate garnets. American Mineralogist, 56, 791–825.

Nye, J.F. (1957) Physical properties of crystals, 322 p. Claredon, Oxford, U.K.

O'Hara, M.J., and Mercy, E.L.P. (1966) Eclogite, peridotite and pyrope from the Navajo country, Arizona and New Mexico. American Mineralogist, 51, 336–352.

Ryerson, F.J., Durham, W.B., Cherniak, D.J., and Lanford, W.A. (1989) Oxygen diffusion in olivine: Effect of oxygen fugacity and implications for creep. Journal of Geophysical Research, 94(B4), 4105–4118.

Schwandt, C.S., Cygan, R.T., and Westrich, H.R. (1993) A thin film approach for producing mineral diffusion couples. Pure and Applied Geophysics, 141, 631–642.

Sharp, Z.D., and Essene, E.J. (1991) Metamorphic conditions of an Archean Core Complex, in the Northern Wind River Range, Wyoming. Journal of Petrology, 32, 241–273.

Sheng, Y.J., Wasserburg, G.J., and Hutcheon, I.D. (1992) Self-diffusion of magnesium in spinel and in equilibrium melts: Constraints on flash heating of silicates. Geochimica et Cosmochimica Acta, 56, 2535–2546.

Shewmon, P. (1989) Diffusion in solids (2nd edition), 246 p. The Minerals, Metals, and Materials Society, Warrendale, Pennsylvania.

Switzer, G.S. (1977) Mineral sciences investigations. Smithsonian Contributions to the Earth Sciences, 19, 1–21.

Thomson, J.A. (1992) A mineralogically and chemically zoned granulite-facies coticule from the Lower Silurian Rangeley Formation, South-Central Massachusetts. Canadian Mineralogist, 30, 393–413.

Tilton, G.R., Schreyer, W., and Schertl, H.-P. (1991) Pb-Sr-Nd isotopic behavior of deeply subducted crustal rocks from the Dora Maira Massif, Western Alps, Italy: II. What is the age of the ultrahigh-pressure metamorphism? Contributions to Mineralogy and Petrology, 108, 22–33.

Vance, D., and O'Nions, R.K. (1990) Isotopic chronometry of zoned garnets: Growth kinetics and metamorphic histories. Earth and Planetary Science Letters, 97, 227–240.

Velde, B., El Moutaouakkil, N., and Ijima, A. (1991) Compositional homogeneity in low-temperature chlorites. Contributions to Mineralogy and Petrology, 107, 21–26.

Wilson, R.G., Stevie, F.A., and MaGee, C.W. (1989) Secondary ion mass spectrometry: A practical handbook for depth profiling and bulk impurity analysis, 165 p. Wiley, New York.

Manuscript received December 23, 1993
Manuscript accepted February 15, 1995